

A PHYSICAL APPROACH FOR DRUG DELIVERY: MAGNETICALLY-DRIVEN NANOSPEARING

A Thesis
Presented to
the Faculty of the Department of Chemical & Biomolecular Engineering
University of Houston

In Partial Fulfillment
of the Requirements for the Degree
Master of Science
in Chemical Engineering

by
Zhen Yang

August 2016

A PHYSICAL APPROACH FOR DRUG DELIVERY: MAGNETICALLY-DRIVEN NANOSPEARING

Zhen Yang

Approved:

Chair of the Committee
Zhifeng Ren, Professor,
Department of Physics

Committee Members:

Richard C. Willson, Professor,
Department of Chemical &
Biomolecular Engineering

Michael Nikolaou, Professor,
Department of Chemical &
Biomolecular Engineering

Suresh K. Khator, Associate Dean,
Cullen College of Engineering

Michael P. Harold, Professor and
Chair, Department of Chemical &
Biomolecular Engineering

ACKNOWLEDGEMENT

This thesis is based on the research conducted at Dr. Zhifeng Ren's lab, which would not have been possible without the help and support from all those including my advisors, my committee members, my colleagues, my friends, and my wife and family.

My very first thanks and deepest gratitude go to my advisor, Dr. Zhifeng Ren: thank you for always supporting me whenever needed, for granting me ultimate freedom in the research, and for inspiring me to do better—if it weren't for you, I'd never been here. Also, many thanks to my co-advisor, Dr. Richard C. Willson. His smart advice, sound opinions, considerable concern and endless support have seen me through this thesis. I have special thanks to Dr. Dong Cai, who led me to the fantastic world of interdisciplinary research of nano-bio-interface, and encouraged me to pursue new ideas and skills. Much thanks to Dr. Michael Nikolaou, whose lectures filled with wisdom and knowledge have inspired my study in mathematics and chemical engineering.

Gratitude also to Dr. Zhonghong Gao, Dr. Yucheng Lan, Dr. Jiming Bao, Dr. Degeng Wang, Dr. Shuo Chen, Dr. Qian Zhang, Dr. Feng Cao, Dr. Chuanfei Guo, Dr. Guoliang He, and Dr. Guoxiong Su, whose assistance proved to be a milestone in the accomplishment of this thesis. It's also my highest privilege to thank Dr. Ching-Wu Chu for his help on the magnetization part in my research. Thanks as always to Dr. Dezhi Wang and Ms. Suqing Li at Dr. Ren's lab.

I would also like to thank all my friends who helped me a lot during the past years. Finally, to my wife and family, thanks for your unconditional love, support and encouragement.

A PHYSICAL APPROACH FOR DRUG DELIVERY: MAGNETICALLY-DRIVEN NANOSPEARING

An Abstract

of a

Thesis

Presented to

the Faculty of the Department of Chemical & Biomolecular Engineering

University of Houston

In Partial Fulfillment

of the Requirements for the Degree

Master of Science

in Chemical Engineering

by

Zhen Yang

August 2016

ABSTRACT

Drug delivery that enables spatial and temporal control is essential to improve pharmacotherapy. The emergence of nanotechnology has spurred the development of drug delivery. Herein, we develop a physics-derived approach, magnetically-driven nanospearing to address challenges associated in drug delivery. Template wetting is employed to formulate a poly- ϵ -caprolactone nanorod-based spear system that incorporates functional agents including amine groups, magnetic nanoparticles, fluorescein molecules, and gold nanorods.

The multifunctional polymeric nanospear provides a promising delivery system for drug delivery. Overall, the amine-group-functionalized surface favors loading of negatively charged molecules, and cellular delivery of ATP is successfully achieved. Gold nanorods functions to enable a photothermally-responsive release behavior for the polymeric spear system. It is also found that the photothermal heating only induces localized structural changes in the polymeric matrix thus triggers surrounded encapsulant release. This localized heating is beneficial to maintain stability of the whole spear system.

This work provides an alternative way for cell internalization and a promising delivery system for targeted delivery and controlled release.

TABLE OF CONTENTS

ACKNOWLEDGEMENT	iv
ABSTRACT	vi
TABLE OF CONTENTS.....	vii
LIST OF FIGURES	ix
LIST OF TABLES	xi
Chapter 1 Introduction	
1.1 Drug Delivery	1
1.2 Nanospearing Technology	4
1.3 Outlines	8
Chapter 2 Fabrication of Nanospears	
2.1 Force Analysis	9
2.2 Poly- ϵ -caprolactone	11
2.3 Template Wetting.....	12
2.4 Layer-by-layer Self-assembly	14
2.5 Composition Characterization	15
2.6 Magnetic Functionalization	17
2.7 Conclusion	18
Chapter 3 Delivery of ATP Molecules	

3.1	Nanospearing across Cells	20
3.2	Conjugation of ATP Molecules	21
3.3	Delivery of ATP Molecules	23
3.4	Gene Transfection	25
3.5	Conclusion	26
Chapter 4 Photothermally-responsive Release		
4.1	Nanospears Functionalization	27
4.2	Thermally-responsive Release	28
4.3	Photothermally-responsive Release	30
4.4	Temperature Measurement	33
4.5	Photothermal Simulation	34
4.6	Conclusion	36
Chapter 5 Conclusion and Outlook		
REFERENCES		40

LIST OF FIGURES

Figure 1. Schematic drawing of nanospearing.....	5
Figure 2. Force analysis of the nanospearing process.....	9
Figure 3. Chemical structure of poly- ϵ -caprolactone.....	12
Figure 4. Template wetting for fabrication of polymer nanorods.....	12
Figure 5. SEM images of PCL nanorods.	13
Figure 6. Construction of core-shell structured PCL nanospears.	14
Figure 7. Optical image of core-shell structured PCL nanospears dispersed in water.	15
Figure 8. FTIR spectrum of surface modified PCL nanorods.	16
Figure 9. Bright field and fluorescent images of FITC-functionalized PCL nanorods. ...	17
Figure 10. Magnetic functionalization of PCL nanospears.	18
Figure 11. Penetration across cells through magnetically-driven nanospearing.....	20
Figure 12. Alexa647-ATP conjugated PCL nanorods.	22
Figure 13. Delivery of Alexa647-ATP into EC9706 cells evaluated via flow cytometry....	23
Figure 14. Delivery of Alexa647-ATP into EC9706 cells.....	24
Figure 15. Transfection of GFP gene into EC9706 cells.	25
Figure 16. Fluorescein-stained PCL nanospears imaged in bright field and FTIC channels.	28
Figure 17. Thermally-responsive release from PCL nanospears delivery system.....	29
Figure 18. Schematic drawing of photothermally-responsive release of PCL nanospears.	30
Figure 19. NIR-induced controlled release of PCL nanospears.	31

Figure 20. Kinetics of NIR-induced release of PCL nanospears.	32
Figure 21. Temperature measurement of gold-nanorods-functionalized PCL nanospears.	33
Figure 22. Simulation of photothermal heating of gold nanorod.....	35

LIST OF TABLES

Table 1. Zeta-potential measurement of core-shell structured PCL nanorods.....	16
--	----

Chapter 1

Introduction

Pharmacotherapy has been impeded by the available administration methods, as most pharmaceutical drugs cannot be directly administrated due to various risk factors^[1-8]. For instance, most synthetic drugs suffer poor solubility in aqueous condition^[9-12] while biomolecular drugs lack of resistance to enzyme-induced degradation^[7, 13-14]. Potential toxicity of therapeutic drugs is also a big concern. In clinic practice, chemotherapy has been a conventional and effective way to combat cancers so far. However, side effects originated from toxicity of chemotherapeutic drugs to normal cells and tissues usually introduce overwhelmed pain and even damage to patients, and thus limit usage of more aggressive therapies^[15-17]. Besides, enhanced permeability and retention effect and reduced immune response are other important factors required into consideration in drug administration^[18-21]. In pharmaceutical industries, compromise is often seen that less active but pharmaceutically optimal compounds become more suitable candidates for development. Such trade-offs may inevitably result in the production of less-ideal drugs^[22]. Thus it becomes necessary to conduct drug delivery research in drug development.

1.1 Drug Delivery

Drug delivery refers to transporting pharmaceutical compounds into designated location within the body as needed to safely achieve its desired therapeutic effect. It generally involves scientific site-targeting within the body and facilitating systemic

pharmacokinetics. The efforts in the area of drug delivery include the development of targeted delivery in which the drug is only active in the targeted area of body (for example, in cancerous tissues), controlled release in which the drug is released over a period of time in a controlled manner from a formulation system. Using drug carriers with drug molecules enclosed or attached is the commonly adopted strategy to deal with the challenges in targeted delivery and controlled release^[23]. Particularly with the emergence and advances in nanotechnology, it has become increasingly appealing to address the issues associated with drug administration^[2, 24-26]. By using nanoscale delivery vehicles, it may be possible to achieve (1) improved delivery of poorly water-soluble molecules; (2) enhanced retention time in the circulation system and reduced immune response; (3) targeted delivery of drugs in a cell- or tissue-specific manner; (3) transcytosis of drugs across tight epithelial and endothelial barriers; (4) delivery of large macromolecule drugs to intracellular sites of action; (5) modified pharmacokinetics of systemic administrated drugs^[10-11, 18, 22, 25, 27-30]. So far, tremendous efforts have been devoted into development of nanoscale delivery systems.

Lipid vesicles, known as liposomes, were the first introduced nanotechnology drug delivery system^[22]. Advanced properties of liposomes include enclosed cavity, modifiable surface and tunable size, which allow liposomes possible to tackle challenges in target delivery and controlled release^[31-32]. For example, enclosed cavity acts as a capsule to load poorly pharmaceutical drugs, such as hydrophobic compounds and macromolecule drugs; surface modification with recognition moieties enables specific interaction with targeted cells that diminishes nonspecific delivery; Tunable size is used to modulate retention time of the carriers in circulation system. So far, a variety of other

organic and inorganic biomaterials for drug delivery have been developed, such as silica nanoparticles^[33], polymeric nanoparticles^[34], dendrimers^[35] and etc. For most of the available drug delivery system, transcytosis of carriers across cell membrane barrier is achieved via endocytosis-induced cell internalization^[36-37]. To initiate this process, drug carriers would have to interact with cell membrane through anchor binding or electrostatic interaction^[26, 38]. Thus, chemistry is usually involved to modify surface of the carriers with functional agents in formulating delivery system. Sparklingly, the anchor binding interaction opens a door to targeted delivery upon using a range of biological targeting moieties, including antibodies^[38-39], targeting peptides^[40], aptamers^[41] and vitamins^[42]. The conjugation of targeted moieties to drug carriers modulates their biodistribution and thus increases local therapeutic concentrations^[43]. For instance, the discovery of new recognition sites has spurred the development of immunotherapies that use antibodies against diseases such as certain cancers^[44]. Such extraordinary emphasis of molecular recognition forms the basis of many biologically derived targeted deliveries.

In yet another important aspect of drug delivery is controlling the release rate of drugs from carrier systems to exhibit the optimal therapeutic concentrations. We have mentioned that drug molecules are enclosed in the carrier chamber or attached on its surface to achieve optimal loading. Degradation of the carrier matrix or failure of the attachment would have the drug molecules released from the delivery system. The central question that has fascinated biomedical researchers from the beginning has therefore been how to design and control material properties to achieve a predictive release response. Strategies widely applied are manipulating the release rates of drugs through synthesis of biocompatible polymers that degrade in predictable ways, or controlling the diffusion

rates of drugs through design of porous matrix^[45]. Poly (lactic-co-glycolic acid) (PLGA) is a great example for development of biodegradable polymers for drug delivery^[8, 34, 46]. Sophisticated engineering of the polymer makes it possible to modulate its degradable rates so that the drug release kinetics could be tuned optimal for pharmacokinetics. The advanced development of PLGA has also inspired vast emergence of other degradable polymers, natural-derived or artificial-synthesized, in application of controlled drug release. Additionally, enormous bioavailability of degradable polymers also spurs the development of polymer-based delivery system for drug delivery. Yet another example is using a reversible chemical linkage, such as disulfide bonds, to formulate drug loading, which enables spatial and temporal control of the drug release^[47-48]. Drug molecules are linked to surface of nanoparticles via disulfide bonds, and thus redox conditions change in the administration environment would break the linkage bonds that release the loaded drug molecules. Thus chemistry has created enormous opportunities to tackle challenges in drug delivery.

1.2 Nanospearing Technology

Today, it has been long interested in biomedical research that how to design and formulate drug carrier systems enabling spatial and temporal control of drug delivery. For decades, researchers have been mostly seeking help from chemistry to address these challenges, and a variety of systems have been developed. As discussed above, chemistry has created vast opportunities for targeted delivery and controlled release. However, the tedious work in chemistry often increases complexity of the formulation and sometimes costs variations from batch to batch production. Beyond those, the basis of chemistry-derived cellular delivery is rooted under the mechanism of endocytosis-induced cell

internalization. Even though the advance in biology development provides sophisticated understanding of endocytosis involved cellular transcytosis, lack of direct control and observation of the process often limits its efficiency on cellular transportation. Moreover, endocytosis involves hazardous conditions, *i.e.*, acidic condition in endosomes and enzyme-catalyzed degradation, which would cost instability on macromolecules based pharmaceutical compounds, such as genes and proteins.

Nowadays, however, the emergence of multidisciplinary development introduces a powerful set of new design concept and technology. Increasingly, scientists are starting seeking physics-derived solutions for controlling biological responses^[43]. For example, methods have been developed that implants electric pulse to pierce holes on cell membrane as a non-fatal invasiveness, through which either exogenous molecules are able to ship into cellular compartment or endogenous molecules can diffuse out of cells^[49-50]. In transdermal drug delivery, microneedles-based delivery system enables transcytosis of drugs across tight epithelial and endothelial barriers via direct penetration, so that efficient delivery is achieved^[51]. Using nanomaterials-induced invasiveness, the pierced holes are confined at nanoscale dimension and thus non-fatal to cell viability.

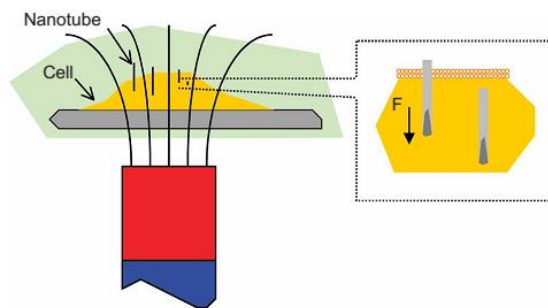


Figure 1. Schematic drawing of nanospearing.

This thesis will focus the interest on nanospearing that is another example of physics-derived technology for cellular internalization. It refers to using magnetic force to drive nanomaterials through cells, acting as spearing, as shown in Figure 1. Nanomaterials, referred to carbon nanotubes in Figure 1, encapsulates a nickel particle at the tips so that their movement is able to be directed by an external magnetic field^[52]. According to the theoretical study of Xin Yi et al., cell uptake of one-dimensional nanomaterials is dominated by a single tension and radius of the nanomaterial and inversely with the membrane bending stiffness^[53]. Thus the uptake follows a near-perpendicular entry mode at small membrane tension while it switches to a near-parallel interaction mode at large membrane tension. In the case of Figure 1, carbon nanotubes possess high aspect ratio and radius of as small as 50 nm, and the active force of magnetic driving aligns the nanotubes perpendicular to cell membrane which overcomes the membrane tension and bending stiffness^[52]. Therefore, we speculate the near-perpendicular entry mode would be favored for uptake of the nanotubes into cells during the nanospearing. In this case, the holes pierced on cell membrane would be confined at the nanoscale size of as small as the radius of the spears implanted during the nanospearing process. Cell membrane, formed through the process of self-assembly and considered as a two-dimensional liquid, could easily restore the tiny damage. David Boal et al. already illustrates in his book that membrane rupture in the case of holes generation is modulated by the competition of membrane-derived surface tension and holes-induced stress tension^[54]. The both tensions are directly correlated to radius of the holes, so that unbounded rupture would only happen when the radius of the holes reaches a threshold value, otherwise, the membrane would still be in metastable state.

Actually, we have already demonstrated in our previous studies that nanospearing is biocompatible to cells, which does not change cell viability or proliferation^[55]. Given that, we showed that nanospearing provided an alternative way for cell internalization that achieved a highly efficient gene transfection in mammalian cells^[52]. Yet another important application was that extraction of intracellular molecules from live cells was achieved through magnetically-driven nanospearing technology^[56]. In these studies, carbon nanotubes modified with a layer of nickel was used as magnetically-drivable nanospears. Under active force of external magnetic field, the nanospearing process was completed in less than 10 minutes. In this short time period, the nanotubes were able to penetrate through cell membranes by the magnetic-driving force. Extending the spearing time would have possibility to drive the nanotubes into and then out of cells. In this case, either exogenous molecules could be shipped into cells or endogenous molecules would be able to transport out of cells, which had both been demonstrated in our previous studies^[52, 56]. Also worth mentioning is that magnetic-field-directed nanospearing makes it possible to drive the magnetic-responsive drug carriers moved into a targeted area of body, and transcytosis of drugs across tight epithelial and endothelial barriers is achievable through nanospearing technology as well.

Given the efficiency of nanospearing for cell internalization, it presents quite promising for drug delivery. However, the controversial debate on carbon nanotubes over its biocompatibility often limits its vast application to address issues associated in biomedical area^[57]. Thus it becomes necessary in the development of nanospearing technology that explores an alternative material suitable for spears formulation. Besides, it still remains unaddressed regarding the control of drug release that associates with

pharmacokinetics in the nanospear-derivative delivery system. All these issues will be sophisticatedly discussed in the following chapters of this thesis. Objective of this thesis is aiming to extend nanospear technology, which enables spatial and temporal control, as a promising approach for drug delivery.

1.3 Outlines

This thesis consists of five chapters. Following the current introductory chapter, chapter 2 presents fabrication of a core-shell structured polymeric nanorod, including fabrication methods, structure characterization and surface functionalization. In chapter 3, application of the polymeric nanorods as nanospears in cellular delivery of ATP small molecules is demonstrated. A photothermally-responsive release behavior from the polymeric nanorods based nanospear delivery system is described in chapter 4. To conclude, chapter 5 gives a summary of the current progress on nanospear technology and outlooks for its promising applications in the biomedical field.

Chapter 2

Fabrication of Nanospears

This chapter presents fabrication of a polymer-based nanospear system, aiming to provide an alternative formulation system rather than carbon nanotubes with more advanced multifunctionality. Herein, template wetting is employed to fabricate the matrix material into nanorod-shaped structure. To advance surface properties, a layer-by-layer self-assembly approach is introduced to pre-coat template pores with layers of macromolecular materials such that a core-shell structured nanospear is constructed. Additionally, magnetic nanoparticles are incorporated into nanospears matrix to impart the system magnetic drivability. Experimental details are discussed in the following content of this chapter.

2.1 Force Analysis

Nanospearing is conducted using magnetic force to direct movement of the nanospears. Figure 2 illustrates two major forces applied on the nanospears during its movement, *i.e.* magnetic force and drag force denoted as F_{mag} and F_d , respectively^[56].

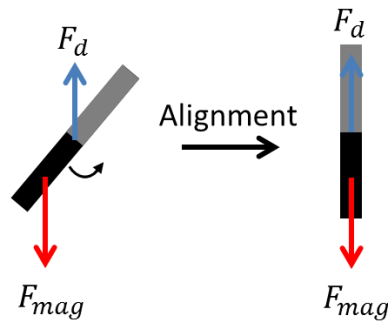


Figure 2. Force analysis of the nanospearing process.

Magnetic force applied on the nanospears is governed by

$$F_{mag} = \frac{1}{2\mu_0} \Delta\chi \cdot V \cdot \nabla B^2, \quad (1)$$

where μ_0 is the magnetic permeability of free space; V and χ are the volume and magnetic susceptibility of the nanospear, respectively, and B is the magnetic field density. As to drag force, it is calculated as

$$F_d = 6\pi \cdot \eta \cdot r \cdot v \cdot K', \quad (2)$$

where η is the viscosity of liquid; r is the radius of the nanospear; v is the velocity of the nanospear in motion, and K' is the shape factor. Net force applied on the nanospear is the summation of the magnetic force (F_{mag}) and the drag force (F_d), as shown as

$$F = F_{mag} - F_d. \quad (3)$$

Efficiency of nanospearing-derived cell internalization is expected to be governed by the net force applied on the nanospears. Given that, it appears favorable for fabrication of nanospears that maximizes the active force of magnetic force, meanwhile, maintains the drag force minimized. Through the governing equations of (1)-(3), a nanospear of large V but small r would be favored for the efficiency of nanospearing. That means a one-dimensional nanostructure of high aspect ratio is preferred. In addition, a high aspect ratio structure would also be favored for a large magnetic field gradient, which would result in a large magnetic force.

Through the above discussion, we can see two criteria for the nanospears in need that includes excellent magnetic drivability and one-dimensional nanostructure. As already discussed in the introduction chapter, matrix material is also a key element for

application of nanospear in drug delivery, and biocompatible and biodegradable polymer based matrix material would be a good candidate for nanospears construction. Overall, a polymeric nanotubes/nanorods-structured nanospear system is chosen and constructed in this chapter.

2.2 Poly- ϵ -caprolactone

Poly- ϵ -caprolactone (PCL), as shown in Figure 3, is a biodegradable polyester with excellent biocompatibility and bioresorbability, and thus has been intensively used in the biomedical fields and a number of drug delivery devices^[58]. Red line in Figure 3 marks the degradable bond of PCL *in vitro* and *in vivo* enzyme catalyzed environment. Additionally, PCL is a hydrophobic and semi-crystalline polymer, which impedes the aqueous molecules access into the PCL bulk and causes a slow degradation rate in *in vitro* and *in vivo*. It makes PCL suitable for a long-term drug treatment. Furthermore, the unique surface-involve erosion makes its degradation highly predictable, giving PCL desirable release vehicles for drugs as release rates can be predetermined. The exceptional blend-compatibility and low melting point (59-64°C) of PCL can also be well manipulated in its controlled release research. For instance, blending with more biodegradable polymers or the enzyme can tune its degradation rate, while the low melting point of PCL can be used to trigger the release with external stimulus^[59-60]. In chapter 4, we will discuss more about that employs its low melting point for controlled release. PCL has been produced into various structures, such as nanoparticles^[61], fibers^[60], films and scaffolds and etc, for biomedical application^[58]. Herein, a PCL-based-nanorod structure is fabricated to construct nanospear system for drug delivery.

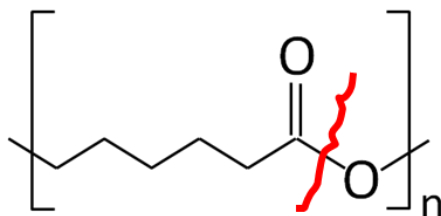


Figure 3. Chemical structure of poly- ϵ -caprolactone.

2.3 Template Wetting

Template wetting, initially reported by Martin CR, is a widely used approach to fabricate nanotubes/nanorods of a broad spectrum of materials, including inorganic and organic materials^[62]. It utilizes the wetting process of liquids including polymer melts or solvents into template pores of high surface energy so that the pores modulate the filled materials to form corresponded tubes/rods structures. The wetting process can either be spontaneously triggered because of capillary tensile force of the solvents itself or externally forced by stimuli like pressure.

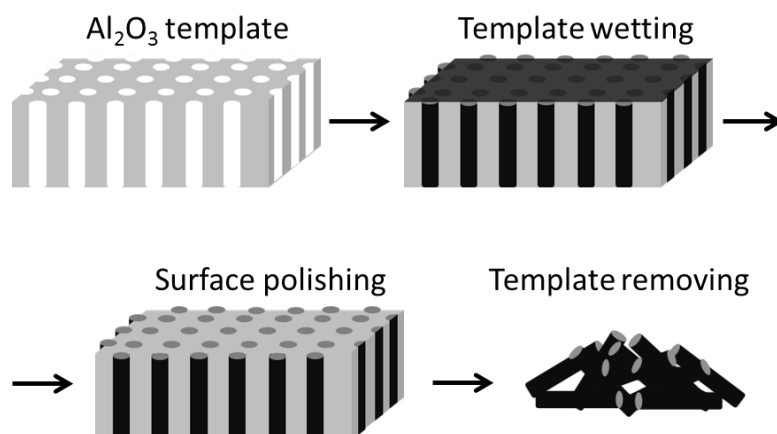


Figure 4. Template wetting for fabrication of polymer nanorods.

Figure 4 presents schematic drawing for the fabrication process by template wetting: porous anodic alumina membrane with highly ordered and uniform nano-scale

pores is used as template; the pores are wetted by tetrahydrofuran (THF) solvent contained 7% w/v PCL, then PCL is resided inside of the template pores to form nanorods-like structures with the evaporation of THF solvent; surface residues of PCL is removed by direct polish; template is removed to release the PCL nanorods by chemical etching in 0.4 M NaOH aqueous solution. In this case, PCL nanorods are obtained.

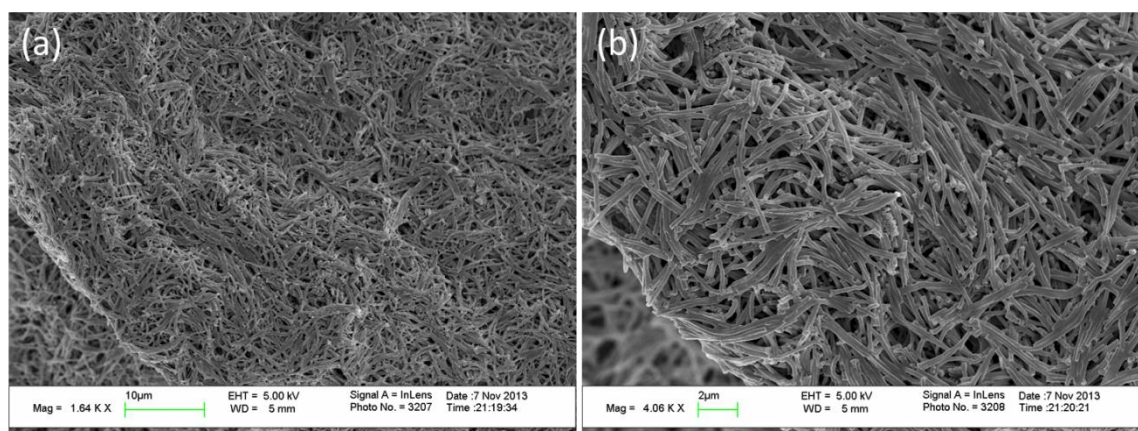


Figure 5. SEM images of PCL nanorods.

As-made PCL nanorods structures are characterized by scanning electron microscopy (SEM), and images are shown in Figure 5. Fabricated PCL nanorods exhibit a uniform diameter of 200 nm with lengths over 6 μm . Through the images, we can also see that yield of the PCL nanorods is quite appreciable. For a template with a 25 mm in diameter and pore density of about 8×10^9 pores per square centimeter, the total yield is as high as about 3.9×10^{10} nanorods per template. Also worth mentioning is that wetting in very small pore sizes could induce the formation of discrete nanoparticles with gradual evaporation of solvent. Recently, Zhang *et al.* reported the formation of various sub-100 nm pure drug nanoparticles by utilizing this phenomenon, which is avoided herein by introducing heat to melt the PCL inside of the template pores, reshaping it along the

dimensions of the pores^[63]. It might explain that lengths of modulated PCL nanorods are relatively smaller than template thickness.

2.4 Layer-by-layer Self-assembly

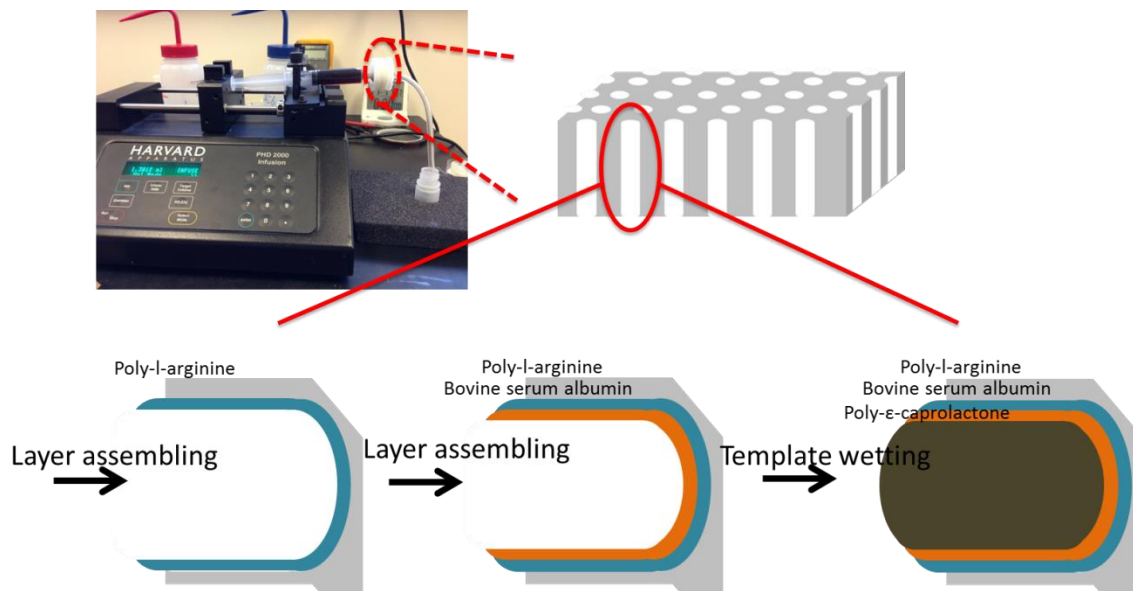


Figure 6. Construction of core-shell structured PCL nanospears.

Hydrophobicity of PCL gives it a good formability in template wetting, however, impedes its direct application in aqueous environment. Thus a core-shell structure is constructed to coat surface of PCL nanorod with layers of hydrophilic biomacromolecules. As illustrated in Figure 6, a layer-by-layer assembly approach is employed to coat the template pores with layers of biomacromolecules. It is an approach developed by Komatsu *et al.* that utilizes electrostatic interaction to assemble molecules along template pores via alternative self-assembly of positive and negative macromolecules layer by layer^[64]. Through this approach, they successfully constructed two kinds of proteins into a nanotube structure. Similarly, we alternatively flow poly-L-arginine (PLA) and bovine serum albumin (BSA) solutions through alumina template

controlled by a syringe pump, as shown in Figure 6. By this way, layers of PLA and BSA are assembled along the template pores to form a nanotube structure. Followed by template wetting as shown in Figure 4, PCL is filled inside of the nanotube of PLA and BSA. So a core-shell structured nanospear is constructed, consisting of hydrophilic biomacromolecules and hydrophobic PCL as shell and core, respectively.

2.5 Composition Characterization



Figure 7. Optical image of core-shell structured PCL nanospears dispersed in water.

Figure 7 presents an optical image of aqueous suspension of PLA/BSA coated PCL nanorods, and frame size of the image is 352 x 265 μm . Through surface modification by layers of PLA/BSA molecules, PCL nanorods become well-dispersed in aqueous solution. Coating of PLA/BSA molecules on PCL nanorods is characterized by other approaches as well, such as Fourier Transform infrared spectroscopy (FTIR) and zeta-potential measurement. Figure 8 shows FTIR spectrum of PLA/BSA coated PCL nanorods in comparison with spectrums of pure PCL and BSA. There are three characterized peaks, *i.e.* $\sim 3300\text{ cm}^{-1}$, ~ 1600 and $\sim 1490\text{ cm}^{-1}$, appeared in PCL nanorods

after PLA/BSA coating, and these peaks are as similar as the peaks in BSA. Analysis of these peaks reveals that $\sim 3300\text{ cm}^{-1}$ attributes to the amine group in BSA, and its amido bond contributes to peaks of ~ 1600 and $\sim 1490\text{ cm}^{-1}$. Since PLA has similar functional groups as BSA, only BSA is used in comparison here.

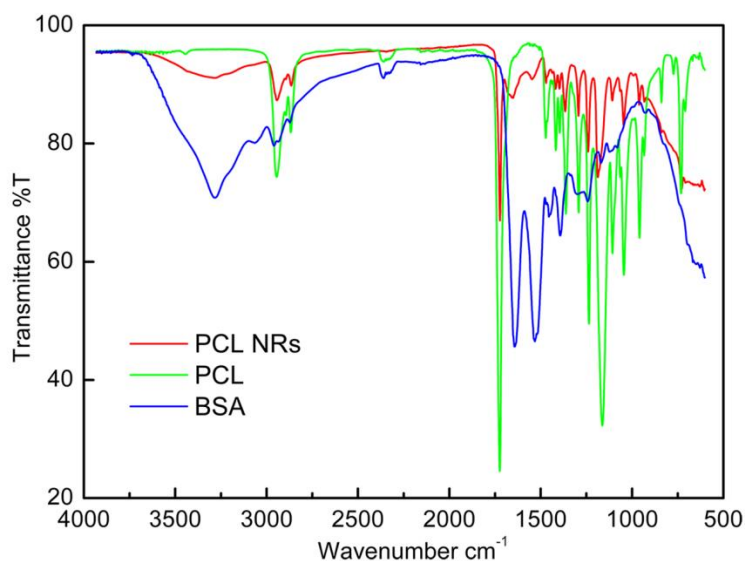


Figure 8. FTIR spectrum of surface modified PCL nanorods.

In addition, outer layer of PLA on PCL nanorods is expected to modulate the nanorods a charged surface with abundant of amine groups. Thus zeta-potential of the PLA/BSA coated PCL nanorods in pH 7.0 condition is measured and listed in Table 1. The positively charged surface in pH 7.0 provides another evidence of the surface functionalization of PLA/BSA molecules.

Table 1. Zeta-potential measurement of core-shell structured PCL nanorods

PCL nanorods	Poly-l-arginine coating
Mobility (M.U.)	3.56
Zeta potential (mV)	47.8 ± 0.5

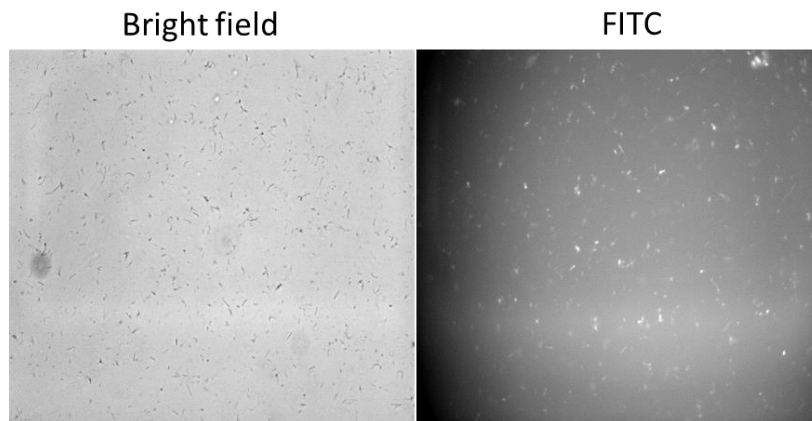


Figure 9. Bright field and fluorescent images of FITC-functionalized PCL nanorods.

The abundant of amine groups carried by PLA macromolecules also imparts the PCL nanorods accessible to chemical functionalization. Fluorescein isothiocyanate (FITC) is a widely used fluorescence dye that is reactive towards nucleophiles, particularly with amine groups on proteins. As shown in Figure 9, PLA/BSA coated PCL nanorods exhibit appreciable fluorescence in FITC channel after fluorescent staining with FITC. The amine group attached on PCL nanorods provides enormous opportunities for functionalizations of the system. It will be further discussed in the following chapter.

2.6 Magnetic Functionalization

Iron oxide is biocompatible and paramagnetic, and has been widely used in diagnosis like magnetic resonance imaging^[65]. In this work, magnetic nanoparticles (MNPs), *i.e.* iron oxide, are incorporated into PCL nanospears to confer magnetic drivability. The MNPs-functionalized PCL nanospears are visualized by SEM (Figure 10a) and transmission electron microscopy (TEM) (Figure 10b), and magnetic drivability is demonstrated by external magnetic attraction (Figure 10c) and quantitatively measured by magnetization response to an external magnetic field (Figure 10d).

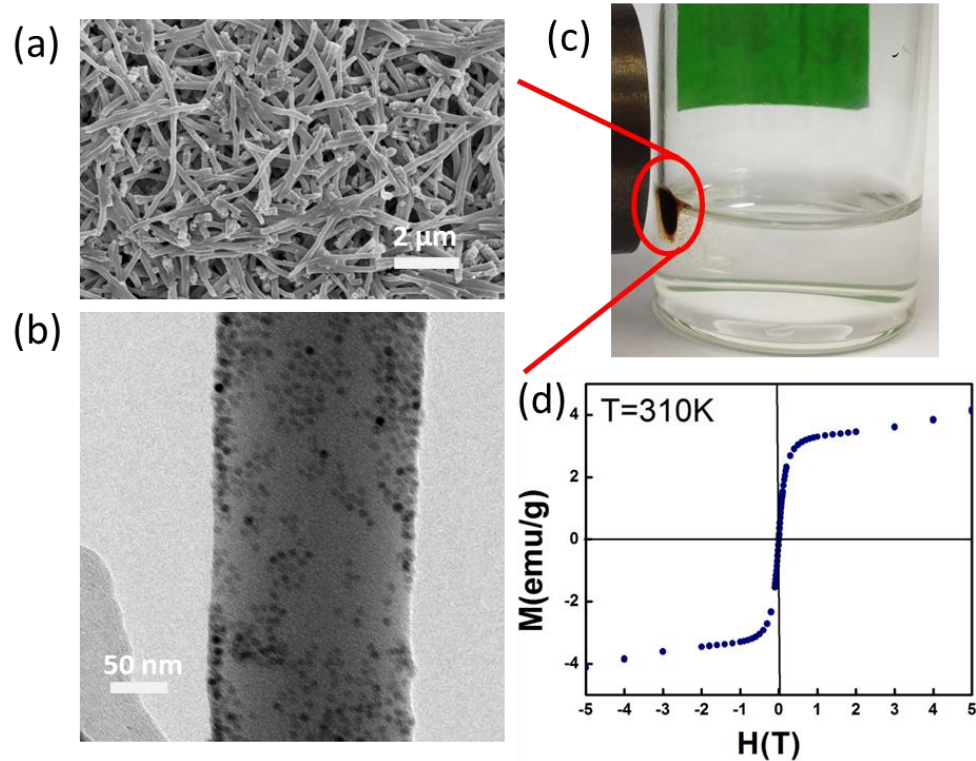


Figure 10. Magnetic functionalization of PCL nanospears.

Functionalization of MNPs is followed by the same procedure as PLA/BSA coating such that MNPs are appeared at the surface of PCL nanorods, as revealed in electron images. Magnetic drivability of the MNPs functionalized PCL nanorods is observed through attraction of the nanorods by an external magnet. And its saturated magnetization is quantitatively measured 4.00 emu g^{-1} at $\sim 0.2 \text{ T}$. In addition, a reversible behavior with no detectable magnetic hysteresis loop displayed in the M - H curve indicates a superparamagnetic property of the MNPs and its functionalized nanospears.

2.7 Conclusion

In summary, we have fabricated a PCL nanorods based nanospear system that is comprised of a core-shell structure and functional agents such as MNPs. The core-shell structure confers the system a hydrophobic core and hydrophilic surface. Meanwhile,

abundant of amine groups carried by the surface PLA molecules gives the system accessibility to various chemical functionalizations. Magnetic drivability imparted from the functional agents of MNPs makes the system applicable for magnetically-driven nanospearing. Overall, the facile formulation of the nanospear system presented in this chapter provides a basis for application practice discussed in chapter 3 and 4.

Chapter 3

Delivery of ATP Molecules

In chapter 2, we present a polymer-based nanospear system through a facile formulation method. This chapter focuses interest on application of this spear system in a drug delivery practice. Adenosine triphosphate (ATP) is a nucleosid triphosphate that transports chemical energy within cells for metabolism. It is used as a substrate in signal transduction pathways by kinases that phosphorylate proteins and lipids. Therefore, it is essential to dissect cellular signal pathways using ATP molecules as tracers. Transcytosis of ATP across cell membrane is energy required, thus it is impermeable into cells. PCL-matrix nanospear system developed in chapter 2 provides a promising carrier system for delivery of ATP molecules into cells. Experimental details of the delivery of ATP molecules are discussed in the following contents of this chapter.

3.1 Nanospearing across Cells

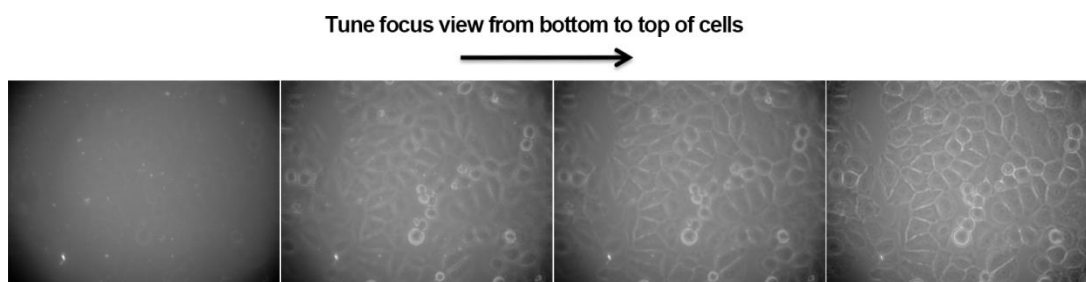


Figure 11. Penetration across cells through magnetically-driven nanospearing.

Magnetically-driven nanospearing imparts an active force on the spear delivery system. When the spears encounter cell membranes, the continuously applied active force would have possibility to overcome energy barriers to penetrate across cells by physically

piercing holes on cell membranes. By this way, delivery of targeted molecules into cells can be achieved. At the beginning of this chapter, we firstly examine the possibility of penetration across cells of the nanospears developed in chapter 2. In section 2.6, it is mentioned that saturated magnetization of the MNPs-functionalized nanospears can be reached at an external magnetic field of ~ 0.2 T. In this work, a commercially available rare-earth magnet of ~ 0.4 T is used to provide a sufficient magnetic field. Esophageal cancer EC9706 cells are seeded and cultured to attach on an image dish. Then MNPs-functionalized PCL-matrix nanospears are supplemented into the culture dish, and they are driven to penetrate across the cells by the magnet located at bottom of the dish. After the nanospearing, the whole system is optically imaged. Bright dots in the images of Figure 11 are functionalized PCL nanospears. To demonstrate the relative location of the nanospears and cells, lens is initially focused at the bottom of cells and then tuned towards its top. We can see in Figure 11 that most of the spears are located at bottom of the dish and even beneath cells, while seldom spears are observed when focus is out of the bottom. It indicates that MNPs-functionalized PCL-matrix nanospears are capable to penetrate across cells.

3.2 Conjugation of ATP Molecules

Now the question has become that how to efficiently load ATP molecules onto the PCL-matrix nanospears system. In section 2.5, zeta-potential measurement reveals a positively charged surface on the core-shell structured nanospears at pH 7.0, which is attributed to abundant of amine groups carried by the PLA coating. On the contrary, ATP carries negative charge at pH 7.0. The loading of ATP molecules can be achieved via electrostatic interaction that directly absorbs ATP molecules onto the surface of PLA-

coated nanospears. To characterize the conjugation, ATP molecules are labeled with Alexa647 dye firstly. Throughout this chapter, Alexa647-labelled ATP molecules (Alexa647-ATP) are used in lieu of ATP molecules. In this case, ATP conjugation and delivery are able to be characterized via fluorescent techniques, including fluorescent microscopy, fluorescent spectrometer and flow cytometry.

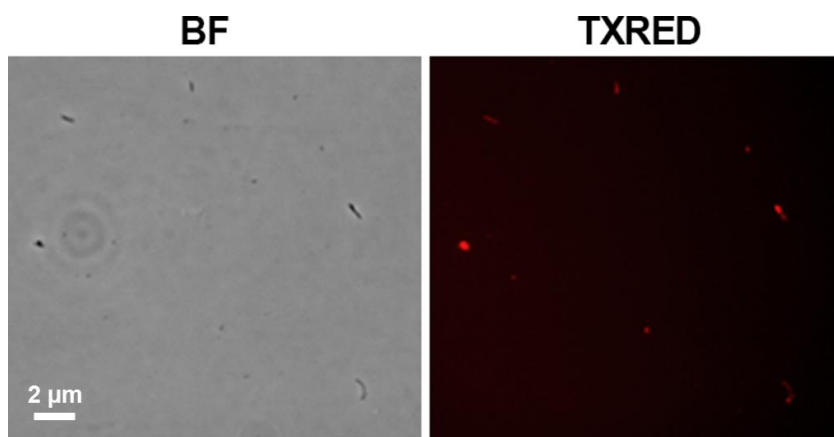


Figure 12. Alexa647-ATP conjugated PCL nanorods.

Figure 12 presents optical images of PCL nanorods after electrostatically loading Alexa647-ATP. The fluorescence exhibited in TXRED channel provides direct evidence of the existence of Alexa647-ATP on the nanorods. Meanwhile, we also quantitatively measure the fluorescence intensity of the conjugated nanorods by a spectrometer, and reveal the loading amount to be $\sim 2 \times 10^5$ dyes per nanorod. Worthy mention is that simply mixing the nanorods into the ATP solution only results in loading efficiency of 4×10^2 dyes per nanorod. In order to enhance the loading efficiency, the mixture is lyophilized such that the ATP molecules precipitate from solution to deposit onto the surface of nanorods. Upon this method, loading efficiency is increased almost 10^3 times.

3.3 Delivery of ATP Molecules

Delivery of ATP molecules is practiced using EC9706 as target cells. Label of Alexa647 provides a tracer for the delivery that would confer cells fluorescence in TXRED channel. Upon loading of Alexa647-ATP molecules, the PCL-matrix nanospears are supplemented into cell culture and pulled down to penetrate cells using the magnet. The whole nanospearing process lasts 10 minutes. Then cells are cultured for another 24 hours such that the delivered Alexa647-ATP molecules would have chances to release from the carriers to stain cells. Flow cytometry and fluorescent microscopy are used to evaluate the delivery efficiency.

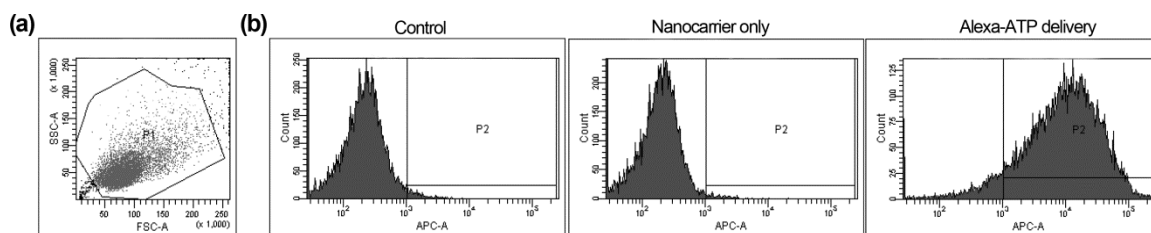


Figure 13. Delivery of Alexa647-ATP into EC9706 cells evaluated via flow cytometry.

In flow cytometry, three groups are compared: cells cultured under normal conditions without any treatment (Control); cells subjected to spearing of bare nanocarriers without any Alexa647-ATP molecules (Nanocarrier only); cells subjected to spearing of Alexa647-ATP conjugated nanocarriers (Alexa-ATP delivery). Control group is used to set the gate that includes majority of the cells under normal conditions, designated to P1. Then histogram graphics of cells in different gates is counted, and P2 counts cells exhibited fluorescence of Alexa647. In Figure 13, we can see that over 90% of cells exhibit fluorescence of Alexa647 in the delivery group while cells subjected to

bare nanocarriers have no fluorescence detected. It shows a successful delivery of ATP molecules into cells using the nanospearing technology.

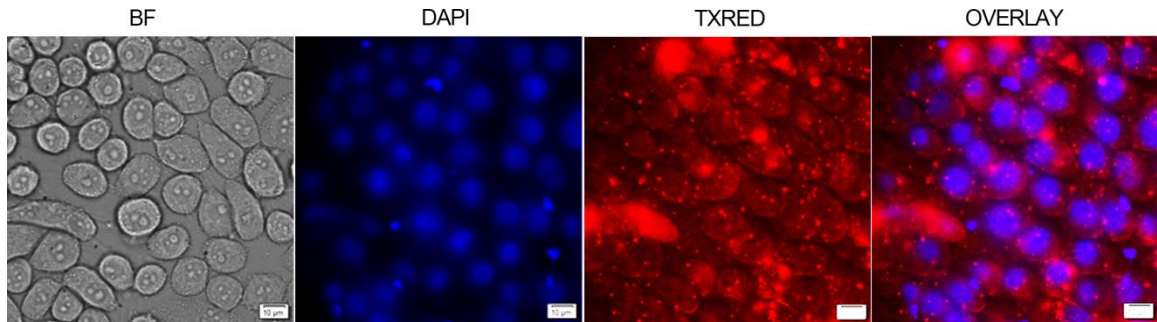


Figure 14. Delivery of Alexa647-ATP into EC9706 cells.

Meanwhile, we also check the fluorescent images of the delivery group. Figure 14 shows the delivery of Alexa674-ATP into EC9706 cells using fluorescent dye of Alexa674 as a tracer. The images are arranged as: BF shows bright-field image of cells subjected to nanospearing; nucleus-stain of DAPI is used to highlight individual cells; TXRED channel reveals the fluorescence emitted from the Alexa674 dye; overlay is the image with DAPI and TXRED channel overlaid. Scale bar is 10 μm in the images. Under the microscopy, most cells exhibit fluorescence in TXRED as shown in Figure 14. It provides additional evidence of the successful delivery of ATP molecules into cells by the nanospearing technology. But it should be noted that lots of red dots (designated to the nanocarriers) are also observed in TXRED channel, and their red fluorescence is much stronger than that of cells. It indicates that only a tiny amount of Alexa647-ATP molecules are delivered into cells, which raises a question to us whether the nanospears observed in Figure 14 are inside or outside of cells.

3.4 Gene Transfection

Poly- ϵ -caprolactone-matrix nanospears are observed contacted with cells in multiple experiments, including Figure 11 and Figure 14. But it is difficult to conclude whether the nanospears are delivered into cells or just stuck onto cell membrane. To address this issue, gene transfection of green fluorescent protein (GFP) is used, because GFP would only get expressed when the gene is delivered inside of cells. GFP gene contained plasmid has the similar negatively charged property as ATP molecules. So similar loading methods as described in section 3.2 is employed to absorb DNA plasmid onto the PCL-matrix nanospears. Absorbance of UV-Visible light reveals the loading amount of plasmid to be 7×10^{-7} ng per nanorod. Then similar nanospearing process is conducted to deliver GFP gene into EC9706 cells as well. After the transfection, cells are continuously cultured for another 24 hours to reach a peak value of GFP expression. Lastly, the expression of GFP is examined using a fluorescent microscopy, as shown in Figure 15.

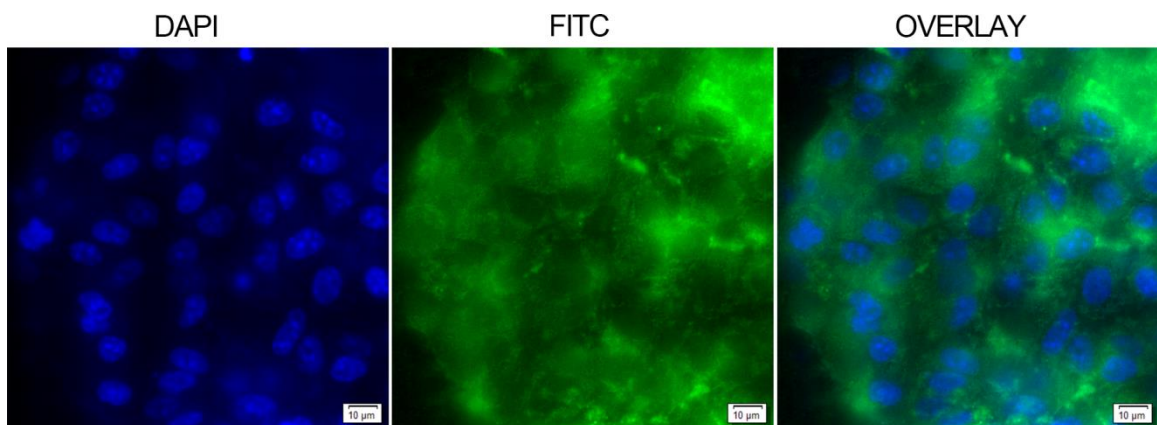


Figure 15. Transfection of GFP gene into EC9706 cells.

Similarly, cells are nucleus-stained with DAPI to highlight individual cells before imaging. As shown in Figure 15, a weak green fluorescence is observed in FITC channel. It answers the question that the PCL-matrix nanospears are capable to deliver cargo into cells. But it is also worthy noted that efficiency of the transfection is relatively low, which corresponds to the low efficiency of ATP delivery. Given these observations, it seems that only partial nanospears get accessed into cells while most of them still are stuck onto cell membrane. The limited efficiency might result from two reasons: (1) magnetization of the nanospears is not sufficient enough to overcome the energy barrier of cell membranes; (2) surface interaction of the polymer-matrix nanospears and cell membrane is too strong that impedes its transcytosis across cell membranes. Correspondingly, magnetization can be enhanced via increasing loading amount of the MNPs, while the surface interaction can be tuned by changing the coating materials of the nanospears. It is important to future work that achieves highly efficient cell internalization in the development of nanospearing for drug delivery.

3.5 Conclusion

In conclusion, this chapter discusses the application of PCL-matrix nanospears in the delivery of ATP molecules. Generally, the nanospears developed in Chapter 2 favors the loading ATP molecules and shows success in its delivery. But the efficiency of delivery is not satisfactory, which requires improved functionalization of the nanospears including its magnetization and surface property.

Chapter 4

Photothermally-responsive Release

Drug delivery that enables spatial and temporal control is essential to improve pharmacotherapy while minimizing undesirable side effects. Magnetically-driven nanospearing has already been demonstrated as a physical approach to achieve cellular internalization that realizes delivery of ATP molecules into cells in chapter 3. In this chapter, we try to extend the nanospearing technology by imparting temporal control of cargo release. As mentioned in section 2.2, properties of PCL including its low melting point (59~64°C) can be manipulated for controlled release research. Meanwhile, formulation method presented in section 2.3, *i.e.* template wetting, makes it possible to feasibly incorporate functional agents, such as gold nanorods and fluorescein molecules, into matrix of the spear system. The embedded gold nanorods would acts as heat actuators that enable photothermally-responsive release behavior for the PCL-matrix spear system. This chapter discusses in detail about the photothermally-responsive release property of the PCL-matrix spear system and its relevant mechanism.

4.1 Nanospears Functionalization

Functional agents, such as fluorescein dye and gold nanorods, are blended into PCL-contained THF solution, and then imbedded into matrix of PCL nanospears by the template wetting approach. Herein, fluorescein dye is used as a surrogate of drug molecules to mimic the controlled release with the PCL-matrix nanospears system, and

gold nanorods function as heat actuators to confer the system photothermally-responsive release.

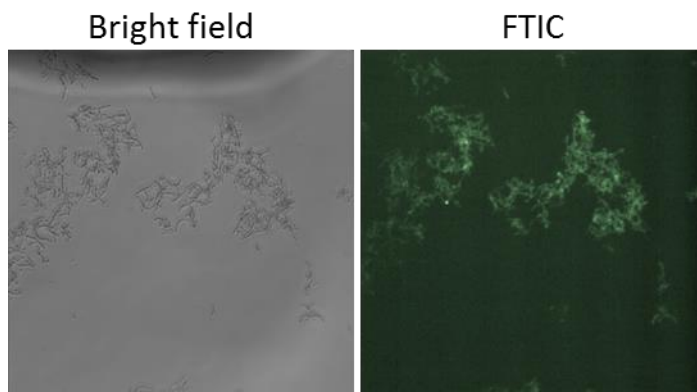


Figure 16. Fluorescein-stained PCL nanospears imaged in bright field and FTIC channels.

Figure 16 shows optical images of fluorescein-stained PCL nanospears. Green fluorescence exhibited in FITC channel shows a successful loading of fluorescein dye in the nanospears carrier system. The loading amount of fluorescein is measured 1 mM. It should be noted that the fluorescence is relatively weak, which might result from fluorescence quenching effect originated from high concentration of fluorescein molecules.

4.2 Thermally-responsive Release

Melting point of PCL is as low as 59-64°C depending on its crystalline ratio, such that this polymer can be systematically manipulated for controlled release^[58]. To demonstrate its thermally-responsive behavior, the fluorescein-loaded PCL nanospears are heated up to the melting point of PCL. Figure 17 shows the release behavior of PCL nanospears delivery system that is controlled by a thermal stimulus. In Figure 17, grey represents the release at room temperature (RT) while white marks the release under

conditions of heating to 55°C. Release fluorescein is quantitatively measured by its absorbance of UV-Visible light and determined by a standard curve of the absorbance versus concentrations. Release quantity at each time interval is normalized to the total loaded amount in Figure 17.

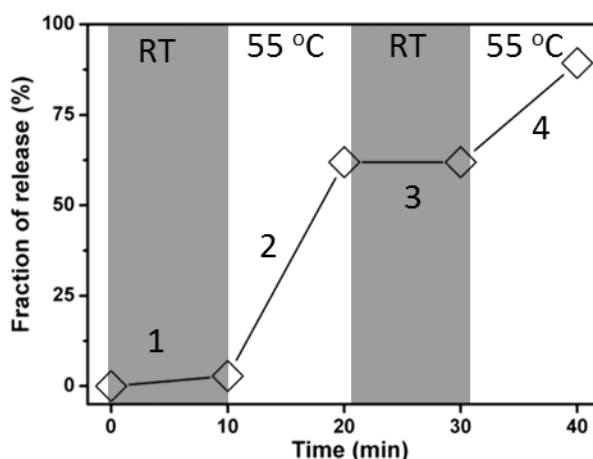


Figure 17. Thermally-responsive release from PCL nanospears delivery system.

We can see that fluorescein is sealed inside the PCL matrix and escapes at a very small diffusion rate (undetectable in UV-Visible absorbance) at RT. Upon heating, the PCL nanostructure is disrupted, and the diffusion rate of embedded fluorescein is accelerated, for instance, ~65% is released in the first cycle of 10 minutes heating and ~25% in the second cycle. Only minor residual fluorescein remains inside the capsule of PCL matrix at the end. This thermally-responsive behavior introduces temperature-stimulus controlled release within the PCL-based delivery system. However, because bulk heating disrupts the nanospear structure, making the carrier inapplicable for systemic drug administration, a better heating mechanism is needed.

4.3 Photothermally-responsive Release

Gold nanoparticles have been widely used in biomedical research, due to its excellent optical properties^[66]. Upon light irradiation, a collective oscillation of free conducting electrons on gold nanoparticles would be induced to create a surface plasmon resonance^[67]. The resonance coupled with the incident electromagnetic field induces plasmonic absorption of light energy and thus generates heat, which is called photothermal effect^[66, 68]. Thus the light-triggered photothermal effects of gold nanoparticles make them excellent heat actuators that are able to induce a thermally-responsive change in the drug carriers to trigger payload release. For example, wrapping polyelectrolyte multilayers on gold nanorods enables light-controlled molecular release^[69]; a liposome-based carrier system is structurally disrupted to release contents by light irradiating on encapsulated gold nanoparticles^[70]; and mesoporous silica nanoparticles break the protection of a capping agent to induce photothermal release^[71].

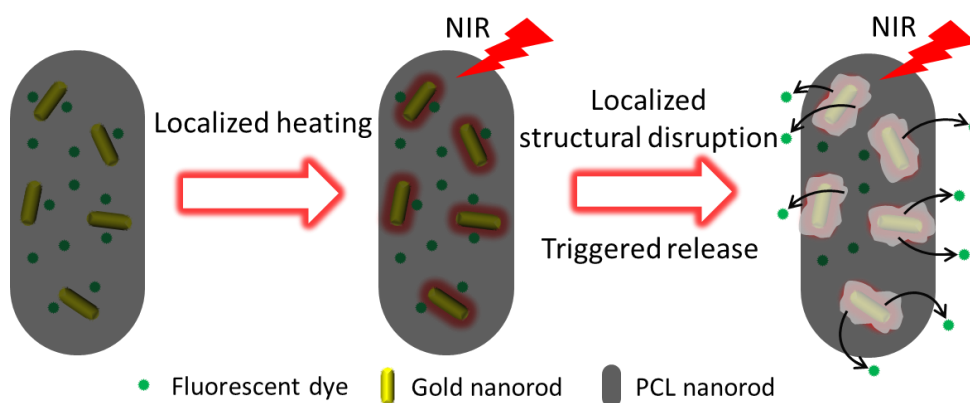


Figure 18. Schematic drawing of photothermally-responsive release of PCL nanospears.

In this work, we incorporate gold nanorods into the PCL-matrix nanospear system to trigger encapsulant release using external light as a stimulus. As illustrated in Figure

18, the system is designed such that fluorescein dye and gold nanorods are co-embedded into PCL nanospearing as described in section 4.1; gold nanorod actuators generate heat confined at its vicinity, inducing only a localized structural change of PCL-matrix nanospears; heat triggers encapsulant release without compromising nanostructure of the delivery system. Resonant light for the gold nanorods used in this work is ~ 830 nm as near-infrared light (NIR). We expect that the NIR-induced heating is only localized at the vicinity of gold nanorods such that bulk temperature of each nanorod is unaffected. Thus, the overall nanostructure of the carriers can be preserved during the triggered release process.

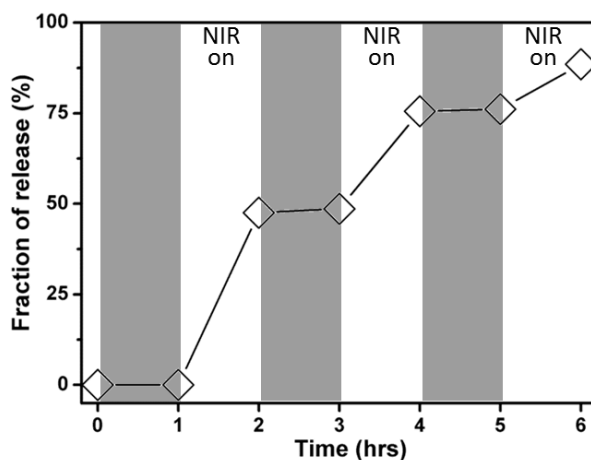


Figure 19. NIR-induced controlled release of PCL nanospears.

Figure 19 shows the experimentally-measured NIR-triggered release profile within the PCL nanospears delivery system. Similarly, the release quantity at each time interval is normalized to the total loaded amount in Figure 19, and grey marks the release without light while white indicates the release upon NIR illumination (NIR on). It is observed that the release of embedded fluorescein dye is triggered and stopped with the start and stop of NIR illumination. This observation corresponds well to the previously

observed thermally-responsive release, but at a smaller diffusion rate. Checking the nanostructure after the release confirms that the overall structure of the spears is intact. In a control experiment, no melting is observed in PCL film samples with gold nanorods embedded upon NIR irradiation. Thus, it is speculated that heat generated by gold nanorods (upon NIR irradiation) induces only localized structural change of PCL, which triggers release of the surrounding fluorescein dye. Upon withdrawing NIR illumination, PCL cools and reforms a sealed capsule for the residual dye and stops further release. The localized effect reduces the risk of carrier instability and also enhances the controllability of release.

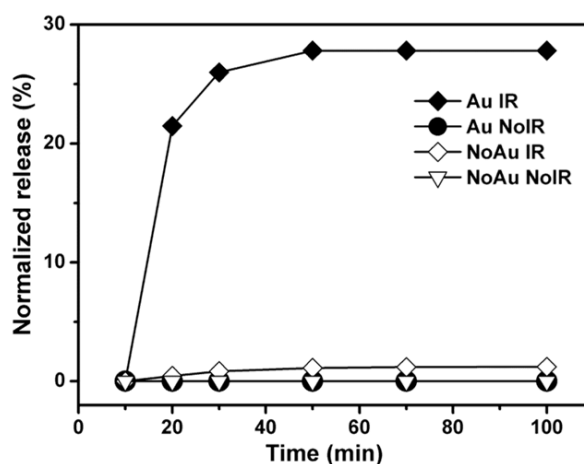


Figure 20. Kinetics of NIR-induced release of PCL nanospears.

Meanwhile, a continuous release profile upon NIR illumination is also quantified, as shown in Figure 20. Four groups are compared: sample incorporates gold nanorods and is subjected to NIR (Au IR); sample incorporates gold nanorods but has no light illumination (Au NoIR); sample is subjected to NIR but has no gold nanorods (NoAu IR); and sample has neither gold nanorods nor light illumination (NoAu NoIR). Also, the released quantity of each time interval is normalized to the loaded amount in Figure 20,

and then the amount released in the first 10 minutes is subtracted per group to normalize the starting level of the four groups. Figure 20 exhibits a pseudo-first-order kinetic diffusion process for the experiment group. Controls lacking either gold nanorods or NIR have barely detectable diffusion rates. These results suggest a photothermally-responsive release behavior of the gold-nanorods-functionalized PCL nanospears delivery system.

4.4 Temperature Measurement

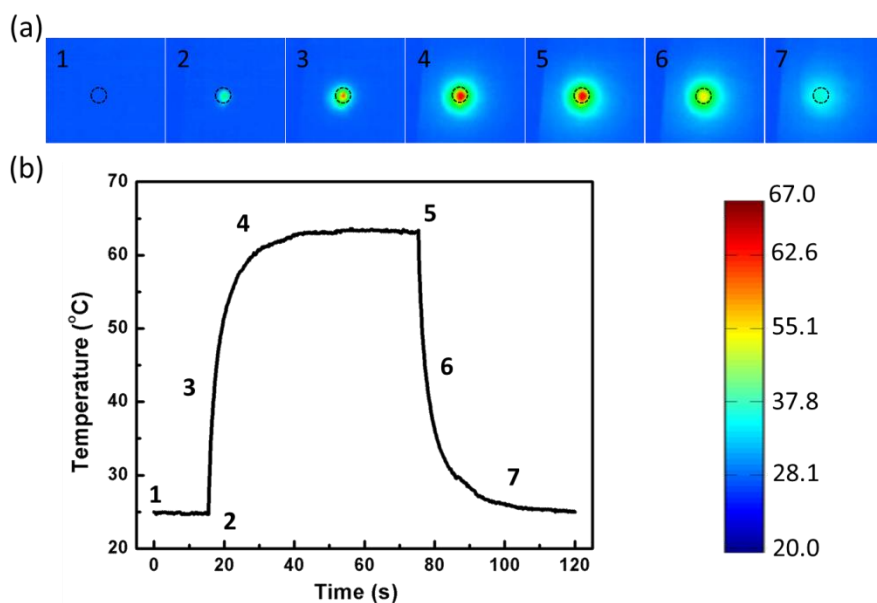


Figure 21. Temperature measurement of gold-nanorods-functionalized PCL nanospears.

To verify the role of gold nanorods in NIR-triggered release of PCL nanospears, we experimentally measure the time-resolved temperature profile of the sample upon NIR irradiation. As shown in Figure 21, the temperature profile is recorded by an infrared camera (A320G, FTIR) with NIR irradiation (Ti-sapphire lase, 2 mm diameter beam, 5 w/cm², 830 nm, Spectra Physics) turned on at 15 seconds and off at 75 seconds. Figure 21 is arranged as: (a) shows time-resolved temperature maps of the sample; (b) presents the corresponding temperature profile of the peak value of the irradiated spot (dotted

circle in (a), 2 mm in diameter); shared color bar represents temperature in degrees Celsius.

In a short period of ~14 seconds irradiation, the temperature measured from the peak value of irradiated spots on gold-nanorods-functionalized PCL nanospears increased from ~25°C to ~67°C, as shown in Figure 21. After turning off the laser, the temperature exponentially decays to ambient temperature. Remarkably, this elevated temperature is already above the melting point of PCL. Yet, it should be noted that the mapped circle in Figure 21a does not indicate the bulk temperature elevation of the circle's highlighted area, but only marks the laser-irradiated position. An infrared camera captures the infrared light that irradiates from designated areas, and these data are interpreted into corresponding temperatures, which might not have to be equivalent to the bulk temperature of the entire circular area. This result indicates that photothermal heating of gold nanorods is sufficient to elevate temperatures as high as 67°C to induce structural changes of PCL.

4.5 Photothermal Simulation

To demonstrate the confined-heating of gold nanorods, we also simulate the temperature distribution along gold nanorod with input parameters identical to the experimental conditions. When gold nanorod is illuminated, the collective oscillation of free electrons on the surface generates surface plasmon resonance. This resonance couples with incident electromagnetic waves, thus inducing an enhanced electric field on the extremities outside the structure. On the contrary, the charge accumulation on the extremities induces a weaker electric field inside the structure^[67-68]. Accordingly, Figure 22a shows a stronger electric field at the inside center of the structure, while the inset

shows a weaker electric field at the outer center of the structure. However, the magnitude of electric fields inside nanorods are much smaller than the enhanced electric fields outside, and the volumetric integration of electric fields inside structures are the main sources of heat, which also corresponded well to the calculated power density on nanorods (Figure 22b). Generated heat is transported from gold surfaces to the surrounding polymer medium, thus increasing temperatures in the corresponding area.

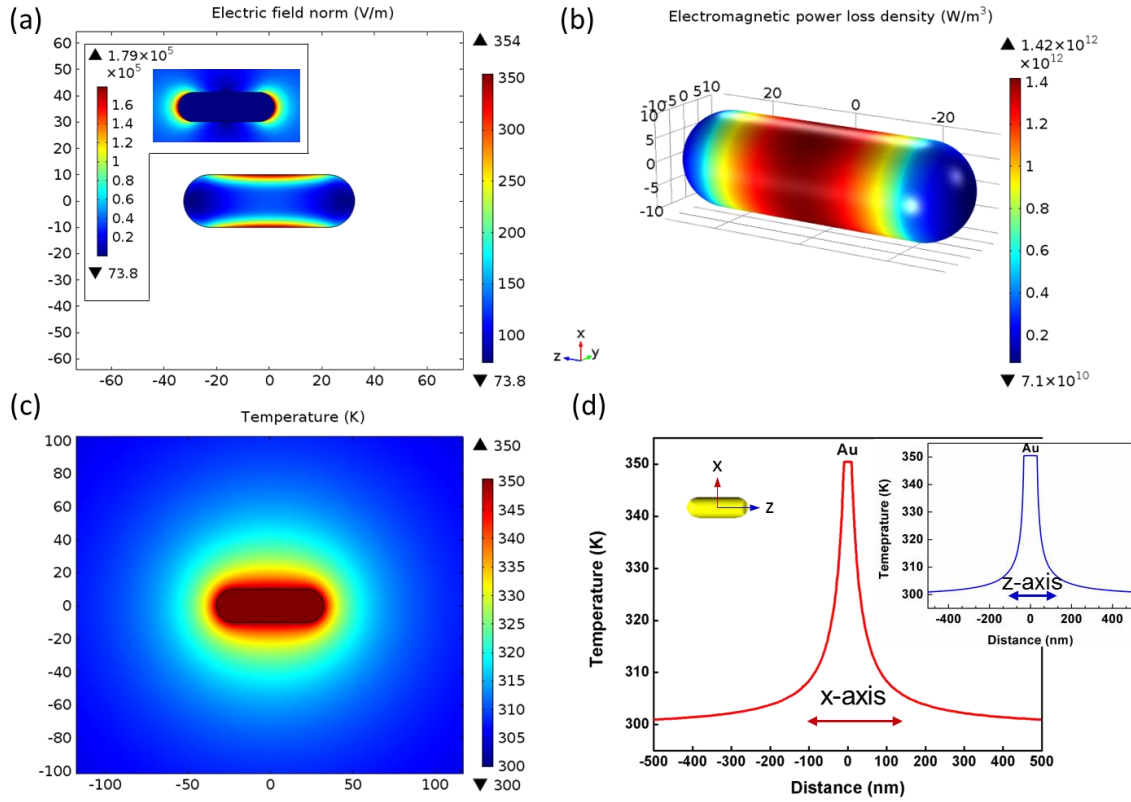


Figure 22. Simulation of photothermal heating of gold nanorod.

Even though the heating power density undergoes spatial variations, the thermal diffusion in gold is so fast that temperature equilibrates quickly and remains almost uniform. Therefore, the steady state temperature increase is determined by the efficiency of thermal diffusion through the surroundings; in this case, the PCL polymer forms a good thermal insulator. Figure 22c shows that the temperature on gold was as high as 77°C (*i.e.*

350 K), and it drops dramatically to room temperature in the vicinity of the nanorod. Outside the vicinity, the temperature in the polymer matrix remains the same as room temperature.

To more clearly illustrate the localized temperature elevation, we plot the temperature profile in Figure 22d and the inset, respectively, with the center point of the nanorod as the origin. This plot shows that the temperature of gold is elevated by up to $\sim 77^{\circ}\text{C}$, and the increase drops dramatically to half at a vicinity of ~ 20 nm along the x-direction and ~ 15 nm along the z-direction of the gold surface. These results strongly support the notion that photothermal heating of gold nanorods would induce only a localized impact on the matrix of the PCL nanospears. Therefore, NIR-responsive release can be imparted to a PCL-based nanospear system by utilizing the photothermal heating of gold nanorods, and the overall nanorod structure is preserved during triggered release.

4.6 Conclusion

In summary, we functionalize the PCL-matrix nanospears with gold nanorods such that the nanospears are conferred a photothermally-responsive release behavior as drug carriers. Surprisingly, the overall nanostructure of the spears is well preserved upon the photothermal heating. Direct temperature measurements indicate that photothermal heating is sufficient to induce structural changes in the PCL matrix. Further simulation of temperature distribution shows that the photothermal heating localizes the temperature elevation around the gold nanorods and has no impact on bulk temperature of the PCL matrix. These data supports a hypothesis that temporal control of encapsulant release is induced by localized structural changes in PCL via photothermal heating. The work

presented in this chapter extends the PCL-matrix nanospears as a promising drug delivery system by imparting it a temporal control of cargo release.

Chapter 5

Conclusion and Outlook

This thesis focuses the study of a physics-derived approach, *i.e.* magnetically-driven nanospearling, for the challenges associated in drug delivery including cellular internalization and controlled cargo release.

At the beginning, a polymeric nanospear delivery system is feasibly formulated via template wetting approach. Matrix material of the nanospear is based on PCL that associates the biocompatibility and biodegradability of drug carriers. Charged layers of PLA and BSA are coated on the surface of PCL nanospear to construct a core-shell structured carrier system by a layer-by-layer self-assembly method. The coating layers of PLA/BSA makes the PCL-matrix nanospear well dispersed in aqueous solution, and abundant of amine groups carried by PLA imparts the nanospear delivery system accessibility to amine-reactive chemistry functionalization. Meanwhile, functional agents, including MNPs, fluorescein dye and gold nanorods, are incorporated into the nanospear delivery system via a facile *in situ* blending strategy in template wetting. This multifunctional polymeric nanospear provides a promising delivery system for the nanospearling-derived drug delivery.

Next, cellular delivery of ATP molecules is conducted using the fabricated multifunctional polymeric nanospear carriers. Amine group coated surface of the nanospear favors the loading of negatively charged molecules, such as ATP molecules and DNA plasmid, via electrostatic absorption. Additionally, it is also found to significantly enhance the loading of ATP molecules onto nanospear carriers that

lyophilizes the mixture. The delivery experiment shows that cellular delivery of ATP molecules is realized through magnetically-driven nanospearing. But the delivery efficiency is not satisfactory. Transfection of GFP gene confirms the capability of magnetically-driven nanospearing in cellular internalization, but also reveals its low efficiency in cargo release by the fabricated polymeric nanospear delivery system.

Meanwhile, we also discuss controlled release property of the gold-nanorods-functionalized PCL nanospears carrier system. A photothermally-responsive release behavior is revealed. To explore its relevant mechanism, we experimentally measure temperature elevation induced by the photothermal-heating of PCL-encapsulated gold nanorods and theoretically simulate the temperature distribution around gold nanorod with electromagnetic wave interaction. Results support a hypothesis that photothermal heating of gold nanorods only induces localized structural changes in PCL thus triggers surrounded encapsulant release. By this way, we extend the nanospearing as a promising delivery system by imparting it a temporal control of cargo release.

Overall, this thesis presents a physics-derived nanospearing technology that is promising in drug delivery. Its properties including facile formulation, capability of cellular internalization and multifunctionalization enable its potential application in targeted delivery and controlled release. But its efficiency of cellular internalization is required further improvement in the future work. Nevertheless, this thesis provides an alternative strategy to address challenges in biomedical research, which is physics-derived approach to direct biological response.

REFERENCES

- [1]. Glass, G., Pharmaceutical Patent Challenges--Time for Reassessment? *Nat Rev Drug Discov* **2004**, 3 (12): 1057-62.
- [2]. Ferrari, M., Cancer Nanotechnology: Opportunities and Challenges. *Nat Rev Cancer* **2005**, 5 (3): 161-71.
- [3]. LaVan, D. A., McGuire, T. F., Langer, R., Small-Scale Systems for in Vivo Drug Delivery. *Nat Biotechnol* **2003**, 21 (10): 1184-91.
- [4]. Luque-Michel, E., Imbuluzqueta, E., Sebastian, V., Blanco-Prieto, M. J., Clinical Advances of Nanocarrier-Based Cancer Therapy and Diagnostics. *Expert Opin Drug Deliv* **2016**: 1744-7593.
- [5]. Whitesides, G. M., The 'Right' Size in Nanobiotechnology. *Nat Biotechnol* **2003**, 21 (10): 1161-5.
- [6]. Zhang, L., Russell, D., Conway, B., Batchelor, H., Strategies and Therapeutic Opportunities for the Delivery of Drugs to the Esophagus. *Crit Rev Ther Drug Carrier Syst* **2008**, 25 (3): 259-304.
- [7]. Wang, M., Zuris, J. A., Meng, F., Rees, H., Sun, S., Deng, P., Han, Y., Gao, X., Pouli, D., Wu, Q., Georgakoudi, I., Liu, D. R., Xu, Q., Efficient Delivery of Genome-Editing Proteins Using Bioreducible Lipid Nanoparticles. *Proc Natl Acad Sci U S A* **2016**, 113 (11): 2868-73.
- [8]. James, R., Manoukian, O. S., Kumbar, S. G., Poly(Lactic Acid) for Delivery of Bioactive Macromolecules. *Adv Drug Deliv Rev* **2016**, (16): 30193-4.

- [9]. Cerpnjak, K., Zvonar, A., Gasperlin, M., Vrecer, F., Lipid-Based Systems as a Promising Approach for Enhancing the Bioavailability of Poorly Water-Soluble Drugs. *Acta Pharm* **2013**, *63* (4): 427-45.
- [10]. Dai, Z., Tu, Y., Zhu, L., Multifunctional Micellar Nanocarriers for Tumor-Targeted Delivery of Hydrophobic Drugs. *J Biomed Nanotechnol* **2016**, *12* (6): 1199-210.
- [11]. Karwal, R., Garg, T., Rath, G., Markandeywar, T. S., Current Trends in Self-Emulsifying Drug Delivery Systems (Seddss) to Enhance the Bioavailability of Poorly Water-Soluble Drugs. *Crit Rev Ther Drug Carrier Syst* **2016**, *33* (1): 1-39.
- [12]. Gupta, S., Kesarla, R., Omri, A., Formulation Strategies to Improve the Bioavailability of Poorly Absorbed Drugs with Special Emphasis on Self-Emulsifying Systems. *ISRN Pharm* **2013**, *2013* (4): 848043-848043.
- [13]. Stremersch, S., Vandenbroucke, R. E., Van Wonterghem, E., Hendrix, A., De Smedt, S. C., Raemdonck, K., Comparing Exosome-Like Vesicles with Liposomes for the Functional Cellular Delivery of Small Rnas. *J Control Release* **2016**, *232*: 51-61.
- [14]. Zuris, J. A., Thompson, D. B., Shu, Y., Guilinger, J. P., Bessen, J. L., Hu, J. H., Maeder, M. L., Joung, J. K., Chen, Z. Y., Liu, D. R., Cationic Lipid-Mediated Delivery of Proteins Enables Efficient Protein-Based Genome Editing in Vitro and in Vivo. *Nat Biotechnol* **2015**, *33* (1): 73-80.
- [15]. O'Hare, M., Sharma, A., Murphy, K., Mookadam, F., Lee, H., Cardio-Oncology Part I: Chemotherapy and Cardiovascular Toxicity. *Expert Rev Cardiovasc Ther* **2015**, *13* (5): 511-8.

- [16]. Zhang, W., Li, C., Shen, C., Liu, Y., Zhao, X., Liu, Y., Zou, D., Gao, Z., Yue, C., Prodrug-Based Nano-Drug Delivery System for Co-Encapsulate Paclitaxel and Carboplatin for Lung Cancer Treatment. *Drug Deliv* **2015**: 1-6.
- [17]. Schwartzberg, L. S., Modiano, M. R., Rapoport, B. L., Chasen, M. R., Gridelli, C., Urban, L., Poma, A., Arora, S., Navari, R. M., Schnadig, I. D., Safety and Efficacy of Rolapitant for Prevention of Chemotherapy-Induced Nausea and Vomiting after Administration of Moderately Emetogenic Chemotherapy or Anthracycline and Cyclophosphamide Regimens in Patients with Cancer: A Randomised, Active-Controlled, Double-Blind, Phase 3 Trial. *Lancet Oncol* **2015**, *16* (9): 1071-8.
- [18]. Pan, D., She, W., Guo, C., Luo, K., Yi, Q., Gu, Z., Pegylated Dendritic Diaminocyclohexyl-Platinum (II) Conjugates as Ph-Responsive Drug Delivery Vehicles with Enhanced Tumor Accumulation and Antitumor Efficacy. *Biomaterials* **2014**, *35* (38): 10080-92.
- [19]. Wang, F., Chen, L., Zhang, R., Chen, Z., Zhu, L., Rgd Peptide Conjugated Liposomal Drug Delivery System for Enhance Therapeutic Efficacy in Treating Bone Metastasis from Prostate Cancer. *J Control Release* **2014**, *196*: 222-33.
- [20]. Chen, W., Meng, F., Cheng, R., Deng, C., Feijen, J., Zhong, Z., Advanced Drug and Gene Delivery Systems Based on Functional Biodegradable Polycarbonates and Copolymers. *J Control Release* **2014**, *190*: 398-414.
- [21]. Li, J., Chu, M. K., Gordijo, C. R., Abbasi, A. Z., Chen, K., Adissu, H. A., Lohn, M., Giacca, A., Plettenburg, O., Wu, X. Y., Microfabricated Microporous Membranes Reduce the Host Immune Response and Prolong the Functional

- Lifetime of a Closed-Loop Insulin Delivery Implant in a Type 1 Diabetic Rat Model. *Biomaterials* **2015**, *47*: 51-61.
- [22]. Shi, J., Votruba, A., Farokhzad, O. C., Langer, R., Nanotechnology in Drug Delivery and Tissue Engineering: From Discovery to Applications. *Nano Lett* **2010**, *10* (9): 3223-30.
- [23]. Allen, T. M., Cullis, P. R., Drug Delivery Systems: Entering the Mainstream. *Science* **2004**, *303* (5665): 1818-22.
- [24]. Peer, D., Karp, J., Hong, S., Farokhzad, O. C., Margalit, R., Langer, R., Nanocarriers as an Emerging Platform for Cancer Therapy. *Nat Nanotechnol* **2007**, *2* (12): 751-60.
- [25]. Davis, M. E., Chen, Z., Shin, D. M., Nanoparticle Therapeutics: An Emerging Treatment Modality for Cancer. *Nat Rev Drug Discov* **2008**, *7* (9): 771-82.
- [26]. Nel, A. E., Madler, L., Velegol, D., Xia, T., Hoek, E. M. V., Somasundaran, P., Klaessig, F., Castranova, V., Thompson, M., Understanding Biophysicochemical Interactions at the Nano-Bio Interface. *Nat Mater* **2009**, *8* (7): 543-57.
- [27]. Farokhzad, O. C., Langer, R., Impact of Nanotechnology on Drug Delivery. *ACS Nano* **2009**, *3* (1): 16-20.
- [28]. Komin, A., Russell, L. M., Hristova, K. A., Searson, P. C., Peptide-Based Strategies for Enhanced Cell Uptake, Transcellular Transport, and Circulation: Mechanisms and Challenges. *Adv Drug Deliv Rev* **2016**, (16): 30186-7.
- [29]. Tu, Y., Zhu, L., Enhancing Cancer Targeting and Anticancer Activity by a Stimulus-Sensitive Multifunctional Polymer-Drug Conjugate. *J Control Release* **2015**, *212*: 95-102.

- [30]. Sun, W., Ji, W., Hall, J. M., Hu, Q., Wang, C., Beisel, C. L., Gu, Z., Self-Assembled DNA Nanoclews for the Efficient Delivery of Crispr-Cas9 for Genome Editing. *Angew Chem Int Ed Engl* **2015**, *54* (41): 12029-33.
- [31]. Gabizon, A., Catane, R., Uziely, B., Kaufman, B., Safra, T., Cohen, R., Martin, F., Huang, A., Barenholz, Y., Prolonged Circulation Time and Enhanced Accumulation in Malignant Exudates of Doxorubicin Encapsulated in Polyethylene-Glycol Coated Liposomes. *Cancer Res* **1994**, *54* (4): 987-92.
- [32]. Samad, A., Sultana, Y., Aqil, M., Liposomal Drug Delivery Systems: An Update Review. *Curr Drug Deliv* **2007**, *4* (4): 297-305.
- [33]. Tang, F., Li, L., Chen, D., Mesoporous Silica Nanoparticles: Synthesis, Biocompatibility and Drug Delivery. *Adv Mater* **2012**, *24* (12): 1504-34.
- [34]. Chan, J. M., Valencia, P. M., Zhang, L., Langer R., Farokhzad, O. C., Polymeric Nanoparticles for Drug Delivery. *Methods Mol Biol* **2010**, *624*: 163-75.
- [35]. Gillies, E. R., Frechet, J. M., Dendrimers and Dendritic Polymers in Drug Delivery. *Drug Discov Today* **2005**, *10* (1): 35-43.
- [36]. Gratton, S. E., Ropp, P. A., Pohlhaus, P. D., Luft, J. C., Madden, V. J., Napier, M. E., DeSimone, J. M., The Effect of Particle Design on Cellular Internalization Pathways. *Proc Natl Acad Sci U S A* **2008**, *105* (33): 11613-8.
- [37]. Sahay, G., Alakhova, D., Kabanov, A. V., Endocytosis of Nanomedicines. *J Control Release* **2010**, *145* (3): 182-95.
- [38]. Qian, Z. M., Li, H., Sun, H., Ho, K., Targeted Drug Delivery Via the Transferrin Receptor-Mediated Endocytosis Pathway. *Pharmacol Rev* **2002**, *54* (4): 561-87.

- [39]. Song, E., Zhu, P., Lee, S. K., Chowdhury, D., Kussman, S., Dykxhoorn, D. M., Feng, Y., Palliser, D., Weiner, D. B., Shankar, P., Marasco, W. A., Lieberman, J., Antibody Mediated in Vivo Delivery of Small Interfering Rnas Via Cell-Surface Receptors. *Nat Biotechnol* **2005**, 23 (6): 709-17.
- [40]. Fawell, S., Seery, J., Daikh, Y., Moore, C., Chen, L. L., Pepinsky, B., Barsoum, J., Tat-Mediated Delivery of Heterologous Proteins into Cells. *Proc Natl Acad Sci U S A* **1994**, 91 (2): 664-8.
- [41]. Farokhzad, O. C., Cheng, J., Teply, B. A., Sherifi, I., Jon, S., Kantoff, P. W., Richie, J. P., Langer, R., Targeted Nanoparticle-Aptamer Bioconjugates for Cancer Chemotherapy in Vivo. *Proc Natl Acad Sci U S A* **2006**, 103 (16): 6315-20.
- [42]. Sato, Y., Murase, K., Kato, J., Kobune, M., Sato, T., Kawano, Y., Takimoto, R., Takada, K., Miyanishi, K., Matsunaga, T., Takayama, T., Niitsu, Y., Resolution of Liver Cirrhosis Using Vitamin a-Coupled Liposomes to Deliver Sirna against a Collagen-Specific Chaperone. *Nat Biotechnol* **2008**, 26 (4): 431-42.
- [43]. Mitragotri, S., Lahann, J., Physical Approaches to Biomaterial Design. *Nat Mater* **2009**, 8 (1): 15-23.
- [44]. Yee, C., The Use of Endogenous T Cells for Adoptive Transfer. *Immunol Rev* **2014**, 257 (1): 250-63.
- [45]. Brayden, D. J., Controlled Release Technologies for Drug Delivery. *Drug Discov Today* **2003**, 8 (21): 976-8.
- [46]. Panyam, J., Labhasetwar, V., Biodegradable Nanoparticles for Drug and Gene Delivery to Cells and Tissue. *Adv Drug Deliv Rev* **2003**, 55 (3): 329-47.

- [47]. Saito, G., Swanson, J., Lee, K. D., Drug Delivery Strategy Utilizing Conjugation Via Reversible Disulfide Linkages: Role and Site of Cellular Reducing Activities. *Adv Drug Deliv Rev* **2003**, 55 (2): 199-215.
- [48]. West, K. R., Otto, S., Reversible Covalent Chemistry in Drug Delivery. *Curr Drug Discov Technol* **2005**, 2 (3): 123-60.
- [49]. Mir, L. M., Bureau, M., Gehl, J., Rangara, R., Rouy, D., Caillaud, J. M., Delaere, P., Branellec, D., Schwartz, B., Scherman, D., High-Efficiency Gene Transfer into Skeletal Muscle Mediated by Electric Pulses. *Proc Natl Acad Sci U S A* **1999**, 96 (8): 4262-7.
- [50]. Geng, T., Bao, N., Sriranganathan, N., Li, L., Lu, C., Genomic DNA Extraction from Cells by Electroporation on an Integrated Microfluidic Platform. *Anal Chem* **2012**, 84 (21): 9632-9.
- [51]. Prausnitz, M. R., Microneedles for Transdermal Drug Delivery. *Adv Drug Deliv Rev* **2004**, 56 (5): 581-7.
- [52]. Cai, D., Mataraza, J., Qin, Z. H., Huang, Z., Huang, J., Chiles, T. C., Carnahan, D., Kempa, K., Ren, Z., Highly Efficient Molecular Delivery into Mammalian Cells Using Carbon Nanotube Spearing. *Nat Methods* **2005**, 2 (6): 449-54.
- [53]. Yi, X., Shi, X., Gao, H., A Universal Law for Cell Uptake of One-Dimensional Nanomaterials. *Nano Lett* **2014**, 14 (2): 1049-55.
- [54]. Boal, D., *Mechanics of the Cell (2nd Edition)*. **2012**.
- [55]. Cai, D., Blair, D. Dufort, F. J., Gumina, M. R., Huang, Z., Hong, G., Wagner, D., Canahan, D., Kempa, K., Ren, Z. F., Chiles, T. C., Interaction between Carbon

- Nanotubes and Mammalian Cells: Characterization by Flow Cytometry and Application. *Nanotechnology* **2008**, *19* (34): 1-10.
- [56]. Yang, Z., Deng, L., Lan, Y., Zhang, X., Gao, Z., Chu, C. W., Cai, D., Ren, Z., Molecular Extraction in Single Live Cells by Sneaking in and out Magnetic Nanomaterials. *Proc Natl Acad Sci U S A* **2014**, *111* (30): 10966-71.
- [57]. Poland, C., Duffin, R., Kinloch, I., Maynard, A., Wallace, W. A. H., Seaton, A., Stone, V., Brown, S., Macnee, W., Donaldson, K., Carbon Nanotubes Introduced into the Abdominal Cavity of Mice Show Asbestos-Like Pathogenicity in a Pilot Study. *Nat Nanotechnol* **2008**, *3* (7): 423-8.
- [58]. Woodruff, M. A., Humacher, D. W., The Return of a Forgotten Polymer-Polycaprolactone in the 21st Century. *Prog Polym Sci* **2010**, *35* (10): 1217-1256.
- [59]. Ahmed, F., Discher, D. E., Self-Porating Polymersomes of Peg-Pla and Peg-Pcl: Hydrolysis-Triggered Controlled Release Vesicles. *J Control Release* **2004**, *96* (1): 37-53.
- [60]. Luong-Van, E., Grondahl, L., Chua, K. N., Leong, K. W., Nurcombe, V., Cool, S. M., Controlled Release of Heparin from Poly(Epsilon-Caprolactone) Electrospun Fibers. *Biomaterials* **2006**, *27* (9): 2042-50.
- [61]. Chawla, J. S., Amiji, M. M., Biodegradable Poly(Epsilon -Caprolactone) Nanoparticles for Tumor-Targeted Delivery of Tamoxifen. *Int J Pharm* **2002**, *249* (1-2): 127-38.
- [62]. Martin, C. R., Nanomaterials: A Membrane-Based Synthetic Approach. *Science* **1994**, *266* (5193): 1961-6.

- [63]. Zhang, J., Li, Y., An, F. F., Zhang, X., Chen, X., Lee, C. S., Preparation and Size Control of Sub-100 Nm Pure Nanodrugs. *Nano Lett* **2015**, *15* (1): 313-8.
- [64]. Qu, X., Lu, G., Tsuchida, E., Komatsu, T., Protein Nanotubes Comprised of an Alternate Layer-by-Layer Assembly Using a Polycation as an Electrostatic Glue. *Chemistry* **2008**, *14* (33): 10303-8.
- [65]. Lu, A. H., Salabas, E., Schuth, F., Magnetic Nanoparticles: Synthesis, Protection, Functionalization, and Application. *Angew Chem Int Ed Engl* **2007**, *46* (8): 1222-44.
- [66]. Jain, P. K., Lee, K., El-Sayed, I. H., El-Sayed, M. A., Calculated Absorption and Scattering Properties of Gold Nanoparticles of Different Size, Shape, and Composition: Applications in Biological Imaging and Biomedicine. *J Phys Chem B* **2006**, *110* (14): 7238-48.
- [67]. Link, S., El-Sayed, M. A., Size and Temperature Dependence of the Plasmon Absorption of Colloidal Gold Nanoparticles. *J Phys Chem B* **1999**, *103* (21): 4212-17.
- [68]. Baffou, G., Quidant, R., Girard, C., Heat Generation in Plasmonic Nanostructures: Influence of Morphology. *Appl Phys Lett* **2009**, *94* (15): 153109.
- [69]. Huang, J., Jackson, K., Murphy, C. J., Polyelectrolyte Wrapping Layers Control Rates of Photothermal Molecular Release from Gold Nanorods. *Nano Lett* **2012**, *12* (6): 2982-7.
- [70]. Paasonen, L., Laaksonen, T., Johans, C., Yliperttula, M., Kontturi, K., Urtti, A., Gold Nanoparticles Enable Selective Light-Induced Contents Release from Liposomes. *J Control Release* **2007**, *122* (1): 86-93.

- [71]. Wu, L., Wu, M., Zeng, Y., Zhang, D., Zheng, A., Liu, X., Liu, J., Multifunctional Peg Modified Dox Loaded Mesoporous Silica Nanoparticle@Cus Nanohybrids as Photo-Thermal Agent and Thermal-Triggered Drug Release Vehicle for Hepatocellular Carcinoma Treatment. *Nanotechnology* **2015**, 26 (2): 025102.

